

Dark blue Čerenkov second harmonic generation in the two-layer-stacked hexagonal periodically poled MgO:LiNbO₃s

Chuanlong Ma (马传龙)¹, Yufei Wang (王宇飞)¹, Lei Liu (刘磊)¹, Xuedong Fan (范学东)¹, Aiyi Qi (齐爱谊)¹, Zhigang Feng (冯志刚)¹, Feng Yang (杨峰)², Qinjun Peng (彭钦军)², Zuyan Xu (许祖彦)², and Wanhua Zheng (郑婉华)^{1,*}

¹State Key Laboratory on Integrated Optoelectronics, Institute of Semiconductors, Chinese Academy of Sciences, Beijing 100083, China

²Technical Institute of Physics and Chemistry, Chinese Academy of Sciences, Beijing 100190, China

*Corresponding author: whzheng@semi.ac.cn

Received November 1, 2013; accepted December 30, 2013; posted online January 24, 2014

We report the dark blue nonlinear Čerenkov radiation by the second harmonic generation (SHG) in a two-layer-stacked hexagonal periodically-poled-MgO:LiNbO₃s (PPMgOLNs). Based on the direct wafer bonding of two target PPMgOLNs rotating around the axis perpendicular to the plane with an angle of 30°, twelve bright spots as twice of those in a single PPMgOLN are shown at each second-harmonic Čerenkov ring. The experimental results agree with the theoretical ones and present a promising application in the fabrication of three-dimensional (3D) PPMgOLNs.

OCIS codes: 050.1940, 190.2620.

doi: 10.3788/COL201412.030501.

The second harmonic generation (SHG) of a laser field has been intensively studied since the emergence of nonlinear optics^[1]. It can be achieved by many different ways, such as the crystal birefringence and the quasi-phase-matching technique, which depend on the fundamental wave polarization, the phase matching, and the type of the nonlinear medium. In quadratic media, these conditions are typically achieved by utilizing the quasi-phase-matching (QPM) technique^[2–7] which involves a periodic modulation of the second-order nonlinearity χ^2 of the material. QPM can be easily obtained in ferroelectric crystals by electric field poling^[8]. The resulting one- or two-dimensional (2D) structures with spatially modulated quadratic nonlinearity are defined as χ^2 nonlinear photonic structures (NPSs). Usually, QPM is realized by collinear propagation of the fundamental frequency (FF) and second-harmonic (SH) beams along the QPM grating vector. Recently, the non-collinear Čerenkov second- or third harmonic generation processes were observed in PPMgOLN^[9], and short-range ordered nonlinear photonic structure has also been reported^[10].

Blue laser radiation is of interest in many various applications, such as display technology, high density optical disk systems, high-resolution printing, and biological applications. In this letter, the dark blue nonlinear Čerenkov radiation by SHG in a two-layer-stacked hexagonal periodically poled Z-cut MgO doped congruent lithium niobate (MgO:CLN) crystal pumped by a femtosecond laser is reported. Based on the direct bonding of the two-layer-stacked PPMgOLNs with an angle offset of 30°, a novel diffraction pattern is observed.

Two interesting diffraction schemes occur when the FF beam vector and the QPM grating vector are non-collinear. As shown in Fig. 1, one is the so-called

Čerenkov second-harmonic generation (CSHG)^[11], which is analogy to the famous Čerenkov effect where a charged particle moves with the velocity exceeding the speed of light in the medium and emits conical radiation. The Čerenkov-type SHG is characterized by the direction of SH emission defined solely by the longitudinal phase matching condition

$$\mathbf{k}_2 \cos \theta - 2\mathbf{k}_1 = 0, \quad (1)$$

where \mathbf{k}_1 and \mathbf{k}_2 are defined as the wave vectors of the fundamental and SH waves, respectively, and θ is the angle of Čerenkov diffraction. The other case is the Raman-Nath diffraction as shown in Fig. 1(b).

In our experiment, the hexagonal PPMgOLNs were fabricated by the standard electric poling of a Z-cut MgO:CLN crystal at room temperature. The pattern of the hexagonal structure is illustrated in Fig. 2(a). The interior angle of the hexagons is 120°, and the side length is 11.46 μm . The domain inverted pattern is shown in Fig. 2(b), which is obtained by dipping the sample in the hydrofluoric acid (HF) for 2 hours. The inverted domains are placed at the corners of the hexagons, and the average diameter is 4.72 μm . The thickness of the sample is 0.42 mm after polishing the both surfaces. Subsequently, two of the same PPMgOLNs are directly bonded together

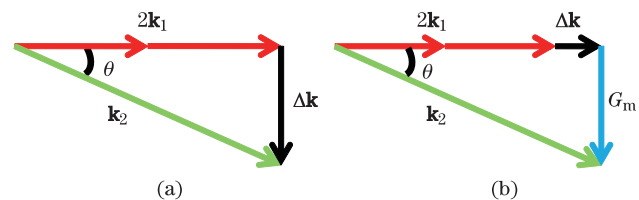


Fig. 1. Phase-matching conditions for (a) nonlinear Čerenkov

and (b) Raman-Nath diffraction.

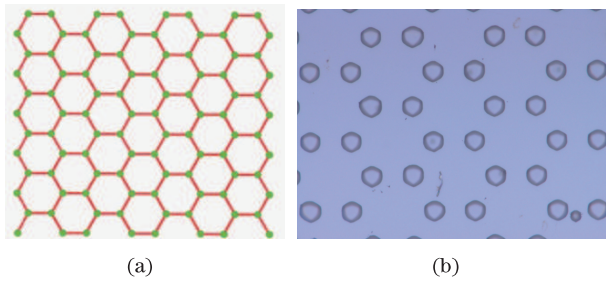


Fig. 2. (a) Pattern of the hexagonal quasi crystal structure; (b) micrograph of the hexagonal quasi periodically poled MgO:CLN crystal.

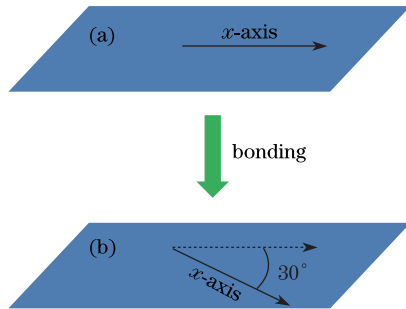


Fig. 3. Schematic diagram of the bonding process. The black solid arrows represent the x -axis direction of the crystals.

with an angle offset of 30° at a low temperature, which is shown in Fig. 3.

The experimental setup is depicted in Fig. 4. The fundamental beam is provided by an 800-nm mode-locked laser (Spectra-Physics, Spitfire Pro). The laser pulse duration, energy, and repetition rate are 100 fs, 1.7 mJ, and 1000 Hz, respectively. The focused beam is perpendicular to the crystal surface with a spot size of about $1200 \mu\text{m}$. Its polarization can be continuously varied by rotating a $\lambda/4$ plate. Because the intensity of the fundamental beam is much stronger than that of the SH diffraction pattern, a screen with a hole in the center to let the fundamental beam pass through lies behind the PPMgOLN, and the emitted SH signal is projected onto a screen and recorded using a charge-coupled device (CCD) camera.

In Fig. 5(a), the diffraction pattern of a single PPMgOLN at SH frequency recorded by CCD camera is shown with just six luminous spots. However, for the two-layer-stacked hexagonal PPMgOLN shown in Fig. 5 (b), twelve luminous spots are obviously observed, which is as twice as that shown in Fig. 5(a). Actually, two rings are obtained in the experiment, but the ring with larger diameter is not recorded in the CCD camera due to its weak intensity. This should be a result of fulfilling the longitudinal phase matching conditions for the Čerenkov type SHG (Fig. 1). The outer ring is formed by the OO-O process, so it is insensitive to the polarization. While the inner ring is formed by the OO-E process, which is generally dominated by the polarization results, so the intensity changes are more obvious. The conical angles in the PPMgOLN of the observed dark blue rings depend on the phase matching relation of the Čerenkov SH radiation rather than the details of the poling patterns. The

relation is described as

$$\cos \theta_{o,e} = 2\mathbf{k}_{1o}/\mathbf{k}_{2o,2e}. \quad (2)$$

The measured conical angles are $\theta_o=66.2^\circ$ and $\theta_e=62.9^\circ$, respectively, which agree well with the theoretical predicted values of $\theta_o=65.9^\circ$ and $\theta_e=61.2^\circ$.

The intensities of the twelve spots in the experimental photograph are not the same, which is due to the polarization of the input beam^[12]. However, the appearance of the twelve super bright spots at the SH Čerenkov ring is believed to be related with the lattice directions in PPMgOLN^[13,14]. The CSHG efficiency is rarely related to the poling patterns, so the same SH blue rings can also be observed in the octagonal quasi crystal structure and rectangular crystal structure poling patterns.

The spectrum characteristics in this CSHG process are concerned. Figures 6(a) and (b) show the spectra of the FF and SH, respectively. Compared with the FF spectrum, rather smooth SH spectra is observed with broad bandwidths, because almost all the FF components satisfying intensity threshold contribute to the SH, leading to a full-band frequency doubling.

In conclusion, two-layer-stacked hexagonal PPMgOLN structure is fabricated at low temperature with an angle

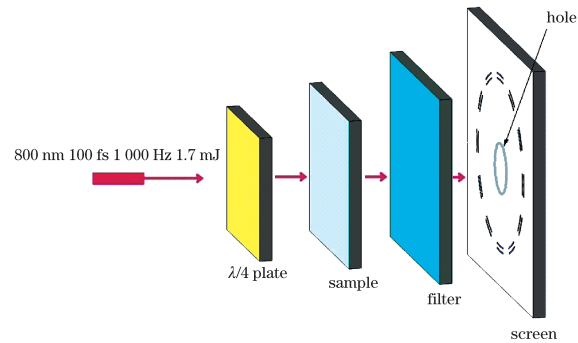


Fig. 4. Schematic diagram of the experimental setup.

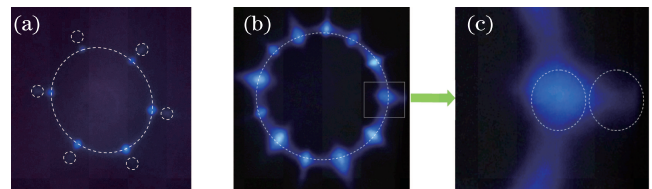


Fig. 5. Experimentally recorded diffraction patterns at the SH frequency for (a) a single PPMgOLN structure and (b) a two-layer-stacked hexagonal PPMgOLN structure. (c) Magnified luminous spots on the inner and the outer ring from (b).

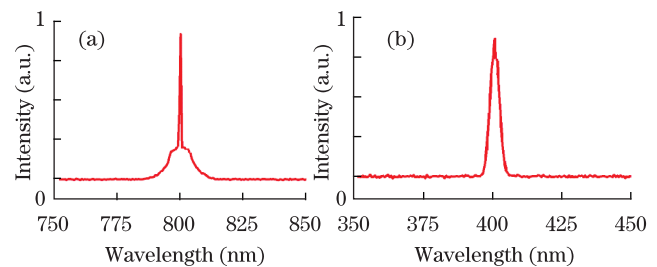


Fig. 6. (a) FF spectrum and (b) SH spectrum from the two-layer-stacked hexagonal PPMgOLN structure.

offset of 30° using directly bonding technology. The dark blue Čerenkov SH ring with twelve luminous spots is well observed from this novel structure. The intensities of the SH rings are stronger if a focusing lens is added. In addition, more luminous spots can be obtained in a multi-bonding PPMgOLN structure, but this work deserves more efforts in the future research. Also the two-layer-stacked hexagonal PPMgOLN structure can be applied in nonlinear microscopy and spectrum.

This work was supported by the National “973” project of China (No. 2012CB933501), the National Natural Science Foundation of China (Nos. 61137003, 61025025, 61021003), and the National “863” Program of China (No. 2013AA030501).

References

1. A. Zembrod, H. Puell, and J. A. Giordmaine, *Opt. Quantum Electron* **1**, 64 (1969).
2. J. A. Armstrong, N. Bloembergen, J. Ducuing, and P. S. Pershan, *Phys. Rev.* **127**, 1918 (1962).
3. S. N. Zhu, Y. Y. Zhu, and N. B. Ming, *Science* **278**, 843 (1997).
4. Y. Chen, J. Zhang, and H. Li, *Chin. Opt. Lett.* **11**, 031601 (2013).
5. Y. Y. Zhu and N. B. Ming, *Opt. Quantum Electron.* **31**, 1093 (1999).
6. A. Fragemann, V. Pasiskevicius, and F. Laurell, *Appl. Phys. Lett.* **85**, 375 (2004).
7. S. Zhang, L. Guo, M. Li, L. Zhang, X. Yan, W. Hou, X. Lin, and J. Li, *Chin. Opt. Lett.* **10**, 071401 (2012).
8. Y. Zhang, Z. Qi, W. Wang, and S. N. Zhu, *Appl. Phys. Lett.* **89**, 171113 (2006).
9. S. M. Saltiel, D. N. Neshev, W. Krolikowski, R. Fisher, A. Arie, and Y. S. Kivshar, *Phys. Rev. Lett.* **100**, 103902 (2008).
10. P. Molina, M. O. Ramirez, B. J. Garcia, and L. E. Bausa, *Appl. Phys. Lett.* **96**, 261111 (2010).
11. Y. Sheng, S. M. Saltiel, W. Krolikowski, A. Arie, K. Koynov, and Y. S. Kivshar, *Opt. Lett.* **35**, 1317 (2010).
12. A. A. Kaminskii, H. Nishioka, K. Ueda, W. Odajima, M. Tateno, K. Sasaki, and A. V. Butashin, *Quantum Electron.* **26**, 381 (1996).
13. S. M. Saltiel, Y. Sheng, N. Voloch-Bloch, D. N. Neshev, W. Krolikowski, A. Arie, K. Koynov, and Y. S. Kivshar, *IEEE J. Quantum Electron.* **45**, 11 (2009).
14. S. M. Saltiel, D. N. Neshev, W. Krolikowski, A. Arie, O. Bang, and Y. S. Kivshar, *Opt. Lett.* **34**, 848 (2009).